

LETTER

Iron partitioning between perovskite and post-perovskite: A transmission electron microscope study

KEI HIROSE,^{1,*} NAOTO TAKAFUJI,¹ KIYOSHI FUJINO,² SEAN R. SHIEH,³ AND THOMAS S. DUFFY⁴

¹Department of Earth and Planetary Sciences, Tokyo Institute of Technology, Meguro, Tokyo 152-8551, Japan

²Division of Earth and Planetary Sciences, Hokkaido University, Sapporo, Hokkaido 060-0810, Japan

³Department of Earth Sciences, University of Western Ontario, London, Ontario N6A 5B7, Canada

⁴Department of Geosciences, Princeton University, Princeton, New Jersey 08544, U.S.A.

ABSTRACT

The effect of iron on the post-perovskite phase transition has been controversial. We have performed direct chemical analyses of co-existing perovskite and post-perovskite that were synthesized from an $(\text{Mg}_{0.91}\text{Fe}_{0.09})\text{SiO}_3$ bulk composition using a laser-heated diamond anvil cell at pressures above 100 GPa and temperatures of 1700–1800 K. Analysis on quenched samples was carried out using the transmission electron microscope (TEM). The results demonstrate that crystalline perovskite grains are enriched in iron compared to adjacent amorphous parts presumably converted from post-perovskite. This indicates that ferrous iron stabilizes perovskite to higher pressures. The ferrous and ferric irons are likely to have competing effects on the post-perovskite phase transition, and therefore the effect of iron may be controlled by aluminum.

Keywords: Perovskite, post-perovskite, iron partitioning, phase transition, D" layer

INTRODUCTION

The recent discovery of MgSiO_3 perovskite to post-perovskite (CaIrO_3 -type) phase transition (e.g., Murakami et al. 2004; Oganov and Ono 2004) has profound implications for the nature and dynamics in the core-mantle boundary region (e.g., Hirose 2006; Lay and Garnero 2007). Strong chemical heterogeneities are likely to exist in this boundary layer, possibly caused by the accumulation of subducted slabs, partial melting in the ultra-low velocity zone, and metal-silicate chemical reactions. It is therefore important to determine the compositional effects on the post-perovskite phase transition. Both experiment and theory show that aluminum stabilizes perovskite relative to post-perovskite (e.g., Tateno et al. 2005; Caracas and Cohen 2005). In contrast, the effect of iron remains unsettled.

X-ray diffraction (XRD) measurements by Mao et al. (2004) demonstrated that the post-perovskite phase transition occurred in $(\text{Mg,Fe})\text{SiO}_3$ at pressures much lower than in pure MgSiO_3 determined earlier by Murakami et al. (2004). This led to the conclusion that iron considerably expanded the stability of post-perovskite to lower pressures. Subsequent TEM studies by Kobayashi et al. (2005) and Auzende et al. (2008) also showed that the Fe/Mg distribution coefficient between post-perovskite and ferropericlasite is higher than that between perovskite and ferropericlasite, $K_D(\text{PPv}/\text{Fp}) > K_D(\text{Pv}/\text{Fp})$, consistent with the XRD studies by Mao et al. (2004). This is supported by theory as well (Caracas and Cohen 2005; Ono and Oganov 2005; Stackhouse et

al. 2006). These calculations show that post-perovskite structure is stable with respect to perovskite in FeSiO_3 end-member at all pressures in Earth's mantle. Contrary to these experimental and theoretical studies, the TEM analyses by Murakami et al. (2005) reported that post-perovskite was depleted in iron compared to perovskite in natural pyrolite. A recent XRD study by Tateno et al. (2007) also demonstrated that $(\text{Mg,Fe})\text{SiO}_3$ perovskite can incorporate more than 75% FeSiO_3 component at deep lower mantle conditions and that iron expands the pressure-temperature (P - T) stability of perovskite relative to post-perovskite, in agreement with the result of Murakami et al. (2005). Thus, there remains important unresolved questions about the behavior of iron in $(\text{Mg,Fe})\text{SiO}_3$ perovskite and post-perovskite and its effect on the phase transition.

Here we performed direct chemical analyses of perovskite and post-perovskite that co-existed in an $(\text{Mg}_{0.91}\text{Fe}_{0.09})\text{SiO}_3$ bulk composition under the TEM. The results demonstrate that perovskite grains include higher amounts of iron than surrounding post-perovskite. This clearly indicates that ferrous iron expands the stability of perovskite to higher pressures, while ferric iron may have the opposite effect.

EXPERIMENTAL METHODS

The sample was synthesized at high P - T using a laser-heated diamond-anvil cell (DAC) by Shieh et al. (2006). The $(\text{Mg}_{1.80}\text{Fe}_{0.18}\text{Al}_{0.01}\text{Ca}_{0.01})\text{Si}_2\text{O}_6$ natural orthopyroxene starting material was directly compressed to 106 GPa in an Ar pressure medium and subsequently heated by a Nd:YLF laser to ~1700–1880 K for a total of 90 min. Platinum was mixed with the sample as a pressure calibrant using the equation of state of Holmes et al. (1989). The size of the hot spot was about 20 μm in diameter. The XRD measurements of this specific sample were reported by Shieh et al. (2006), and demonstrated the co-existence of perovskite and post-

* E-mail: kei@geo.titech.ac.jp

perovskite phases. The peaks from post-perovskite were more intense than those of perovskite. The apparent synthesis pressure is lower than observed in MgSiO_3 composition, in which the phase transition occurred between 114 and 127 GPa (Murakami et al. 2004). However, pressure was not measured in situ at high P - T in the present experiments. The pressure may have been higher by 10–15% at high temperature due to a contribution of thermal pressure (e.g., Murakami et al. 2004). Also, pressures could be affected by chemical reaction of Pt and Fe.

The sample was decompressed at room temperature and XRD patterns were measured at various pressures. Below ~80 GPa, integrated diffraction peaks from post-perovskite became weak and broad but were still detectable down to 12 GPa. At 1 bar, a single weak peak near the expected location of the (022) line was still observed, indicating possible partial quench of the post-perovskite phase, but this peak was considerably weaker when the sample was re-examined one week after the initial experiment, suggesting progressive disordering over this time period. The diffracted intensity of post-perovskite below 80 GPa consisted of a small number of discrete spots on the image plate detector. Furthermore, the peak consistent with (022) at 1 bar was detected only at a single location in the sample, and moving a few micrometers away caused the peak to disappear. Thus, any crystalline material was likely to be highly localized, and the vast majority of post-perovskite material was apparently amorphous.

The sample was recovered from the DAC and subsequently Ar ion-thinned with a low-voltage and low-current beam, using a cooling stage to minimize heating (see Fujino et al. 1998 for details). This prevented perovskite from converting to an amorphous phase during the thinning process. We examined two separate areas of this thin foil under the JEOL JEM-2010 TEM operating at 200 kV. Each area was $\sim 1 \mu\text{m} \times \sim 500 \text{ nm}$ large, and two regions were separated by about 5 μm . As shown in Figure 1, a crystalline phase was surrounded by an amorphous material. As discussed above, the post-perovskite phase was mostly to completely amorphous after quench and any residual crystalline post-perovskite likely degraded over the time interval of more than six months prior to TEM analysis or during ion thinning. Thus, the crystalline phase should represent perovskite, and presumably the majority of the unstructured part was originally post-perovskite. The size of perovskite grains was typically 50 to 100 nm. Chemical analyses of the crystalline (perovskite) and amorphous (mostly post-perovskite) portions were carried out with a NORAN Instruments/Voyager II energy-dispersive X-ray spectroscopy (EDS) analytical system attached to the TEM. We calculated the compositions from measured X-ray intensities using experimentally determined k -factors (Cliff and Lorimer 1975). All the analyses were made only for extremely thin parts where electron transparency was greater than 94%, though we avoided the very edge of the thinned sample. These analytical procedures were the same as those in Hirose et al. (2005).

RESULTS

We obtained the EDS analyses of 14 perovskite grains and 17 amorphous points from two discrete areas (Table 1). The results show that amorphous parts contained lesser amounts of iron than

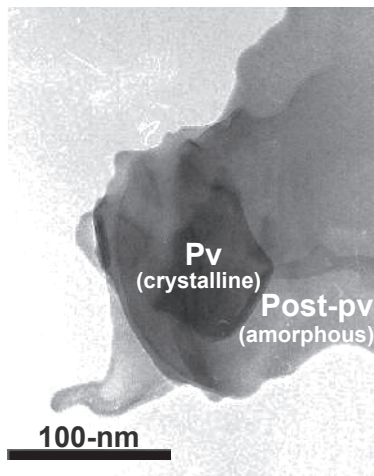


FIGURE 1. TEM microphotograph of the sample recovered from DAC. The crystalline perovskite is surrounded by amorphous material presumably converted from post-perovskite.

the co-existing crystalline perovskite. The average $\text{Mg}/(\text{Mg} + \text{Fe})$ molar ratio $\times 100 (=X_{\text{Mg}})$ of the former was 93.5 ± 1.2 (93.4 ± 1.4 for area 1 and 93.5 ± 1.0 for area 2), whereas the average X_{Mg} of the latter was determined to be 89.1 ± 1.8 (88.5 ± 1.9 for area 1 and 89.7 ± 1.7 for area 2) (Fig. 2). A couple of analyses of the amorphous portions in area 2 showed exceptionally high iron contents (low X_{Mg}), more than co-existing perovskite grains (Fig. 2), suggesting that some part of the amorphous region could be originally perovskite. We did not recognize a systematic difference in thickness between the crystalline phase and the surrounding unstructured part under the TEM. A metallic phase was not observed in our sample.

Present analyses do not indicate the $\text{Fe}^{2+}/\text{Fe}^{3+}$ ratio, but the system was Al free and therefore ferrous iron should be dominant. The $\text{Fe}^{3+}/\Sigma\text{Fe}$ ratio was previously determined to be 0.10 for perovskite at 99 GPa and 0.11–0.13 for post-perovskite at 128–129 GPa in Al-free systems, based on electron energy-loss near-edge structure (ELNES) spectroscopy measurements (Ohta et al. 2008a; Sinmyo et al. 2008). The Fe^{3+} abundance could be about 10% of the total iron in our sample.

EFFECT OF IRON ON POST-PEROVSKITE PHASE TRANSITION

These results indicate that perovskite is enriched in ferrous iron compared to co-existing post-perovskite. This means that Fe^{2+} should expand the P - T stability of $(\text{Mg,Fe})\text{SiO}_3$ perovskite relative to that of post-perovskite. This is consistent with the recent XRD study by Tateno et al. (2007), which demonstrated that the perovskite to post-perovskite phase transition occurred in $(\text{Mg}_{0.5}\text{Fe}_{0.5})\text{SiO}_3$ at pressures higher than in the Mg end-member. Theory has repeatedly suggested the opposite (Caracas and Cohen 2005; Ono and Oganov 2005; Stackhouse et al. 2006). However, theoretical calculations on the stability of iron-bearing silicates are still challenging (e.g., Cococcioni and de Gironcoli 2005). Experimental determinations of the stability of $(\text{Mg,Fe})\text{SiO}_3$ post-perovskite by Mao et al. (2004) and Shieh et al. (2006)

TABLE 1. Molar compositions of co-existing crystalline and amorphous parts

Crystalline (perovskite)					Amorphous (mostly post-perovskite)				
Si	Mg	Fe	cation sum	X_{Mg}	Si	Mg	Fe	cation sum	X_{Mg}
Area 1									
0.977	0.960	0.087	2.024	91.7	1.002	0.929	0.067	1.998	93.3
0.962	0.980	0.116	2.058	89.4	0.992	0.940	0.075	2.007	92.6
0.993	0.877	0.140	2.010	86.2	1.002	0.953	0.043	1.998	95.7
0.994	0.903	0.109	2.006	89.2	0.999	0.923	0.080	2.002	92.0
0.994	0.903	0.109	2.006	89.2	0.995	0.928	0.081	2.004	92.0
0.981	0.910	0.128	2.019	87.7	1.028	0.882	0.062	1.972	93.4
1.000	0.871	0.139	2.010	86.2	0.996	0.937	0.071	2.004	93.0
			average	88.5	1.005	0.944	0.045	1.994	95.4
								average	93.4
Area 2									
1.004	0.907	0.084	1.996	91.5	1.006	0.932	0.057	1.994	94.2
0.987	0.916	0.109	2.013	89.4	1.013	0.921	0.054	1.987	94.5
1.016	0.880	0.089	1.984	90.8	1.012	0.920	0.056	1.988	94.3
0.975	0.935	0.114	2.025	89.1	0.991	0.916	0.102	2.009	90.0*
0.989	0.899	0.123	2.011	88.0	0.992	0.940	0.077	2.008	92.4
0.954	1.001	0.091	2.046	91.7	1.000	0.918	0.082	2.000	91.8
0.941	0.977	0.140	2.059	87.5	1.019	0.901	0.060	1.981	93.8
			average	89.7	0.983	0.966	0.067	2.017	93.5
					0.984	0.894	0.138	2.016	86.6*
								average	93.5

* These two amorphous parts contain exceptionally high iron content (low X_{Mg}), more than co-existing perovskite grains (Fig. 2), suggesting that they were originally perovskite. Average X_{Mg} was calculated without these two data.

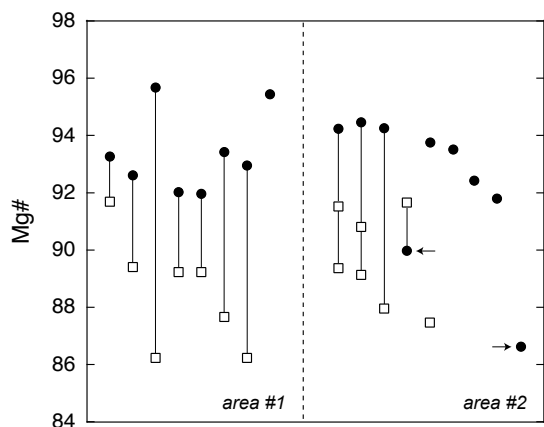


FIGURE 2. Mg/(Mg + Fe) molar ratio $\times 100$ ($\equiv X_{Mg}$) of co-existing crystalline perovskite (open squares) and amorphous parts (solid circles). The majority of amorphous portion was originally post-perovskite. A couple of analyses show exceptionally low X_{Mg} (circles with arrow), suggesting that part of the amorphous portion was converted from perovskite. The tie-lines indicate the analyses of adjacent grains.

included large uncertainties in pressure estimates because pressures were measured at room temperature in both the studies. The TEM works by Kobayashi et al. (2005) and Auzende et al. (2008) possibly had a difficulty in obtaining equilibrium Fe^{2+} -Mg distribution coefficients, because of the heterogeneity of the iron content in a laser-heated sample (Hirose and Sinmyo 2007).

Both perovskite and post-perovskite contain both ferrous and ferric iron in natural Al-bearing systems (e.g., Frost and Langenhorst 2002; Sinmyo et al. 2006). In contrast to Fe^{2+} , Fe^{3+} likely stabilizes post-perovskite to lower pressures. A previous experimental study reported the $CaIrO_3$ -type Fe_2O_3 phase as low as 60 GPa (Ono and Ohishi 2005). The theoretical calculations by Zhang and Oganov (2006) predicted that Fe^{3+} reduces the pressure of $MgSiO_3$ post-perovskite phase transition considerably. This is consistent with earlier experimental results on pyrolite and MORB compositions. Perovskite undergoes phase transition to post-perovskite in pyrolite at pressures equivalent to that in Mg end-member (Ohta et al. 2008b). This could be the result of competing effects of ferrous iron and aluminum (positive) and ferric iron (negative). In addition, Al-enriched post-perovskite contained large amounts of ferric iron ($Fe^{3+}/\Sigma Fe = 0.65$) in a MORB composition (Sinmyo et al. 2006), and the post-perovskite phase transition occurred in MORB at 4 GPa lower pressure than in pure $MgSiO_3$ (Ohta et al. 2008b). However, the effect of ferric iron has not been demonstrated explicitly by experiment. Nishio-Hamane et al. (2007) reported that the incorporation of $Fe^{3+}AlO_3$ stabilizes perovskite to higher pressures.

By virtue of its location, the D'' region is a thermal, chemical, and mechanical boundary layer at the bottom of the mantle. Chemical heterogeneity likely exists in this boundary layer, especially in iron content, caused by accumulation of dense components above the core-mantle boundary (CMB). Such dense materials could have been derived by a deep subduction of basaltic oceanic crust (Hirose et al. 2005; Ohta et al. 2008b) or banded iron formations (BIFs) (Dobson and Brodholt 2005).

Partial melting and crystallization, which has been suggested to occur at the ultra-low velocity zone right above the CMB, can cause extensive enrichment/depletion of iron (Hirose and Fei, 2002; Ito et al. 2004). Core-mantle chemical reactions also produce variations in iron content at the base of the mantle (Takafuji et al. 2005; Asahara et al. 2007; Ozawa et al. 2008). Such heterogeneities in iron content affect the depth of post-perovskite phase transition in the D'' layer.

The effect of iron on the stabilities of perovskite and post-perovskite may depend strongly on the Fe^{3+}/Fe^{2+} ratio, if ferrous and ferric iron have opposite effects. The ELNES spectroscopy measurements on both Al-free (Ohta et al. 2008a; Sinmyo et al. 2008) and Al-enriched post-perovskite (Sinmyo et al. 2006) suggest that the concentration of Fe^{3+} increases with increasing Al^{3+} , similarly to the case of perovskite (Lauterbach et al. 2000; Frost and Langenhorst 2002). Aluminum is therefore the key control on the effect of iron.

ACKNOWLEDGMENTS

We thank the reviewers for helpful comments on the manuscript. R. Sinmyo is acknowledged for discussion. This work was supported by research grants from the JSPS to K.H. and from the NSF to T.D. Portions of this work were performed at GeoSoilEnviroCARS (Sector 13), Advanced Photon Source (APS), Argonne National Laboratory. GeoSoilEnviroCARS is supported by the NSF and Department of Energy—Geosciences.

REFERENCES CITED

- Asahara, Y., Frost, D.J., and Rubie, D.C. (2007) Partitioning of FeO between magnesio-wüstite and liquid iron at high pressures and temperatures: Implications for the composition of the Earth's outer core. *Earth and Planetary Science Letters*, 257, 435–449.
- Auzende, A.-L., Badro, J., Ryerson, F.J., Weber, P.K., Fallon, S.J., Addad, A., Siebert, J., and Fiquet, G. (2008) Element partitioning between magnesium silicate perovskite and ferropericlasite: new insights into bulk lower-mantle geochemistry. *Earth and Planetary Science Letters*, 269, 164–174.
- Caracas, R. and Cohen, R.E. (2005) Effect of chemistry on the stability and elasticity of the perovskite and post-perovskite phases in the $MgSiO_3$ - $FeSiO_3$ - Al_2O_3 system and implications for the lowermost mantle. *Geophysical Research Letters*, 32, L16310, DOI: 10.1029/2005GL023164.
- Cliff, G. and Lorimer, G.W. (1975) The quantitative analysis of thin specimens. *Journal of Microscopy*, 103, 203–207.
- Coccoccioni, M. and de Gironcoli, S. (2005) Linear response approach to the calculation of the effective interaction parameters in the LDA + U method. *Physical Review B*, 71, 035105.
- Dobson, D.P. and Brodholt, J.P. (2005) Subducted banded iron formations as a source of ultralow-velocity zones at the core-mantle boundary. *Nature*, 434, 371–374.
- Frost, D.J. and Langenhorst, F. (2002) The effect of Al_2O_3 on Fe-Mg partitioning between magnesio-wüstite and magnesium silicate perovskite. *Earth and Planetary Science Letters*, 199, 227–241.
- Fujino, K., Miyajima, N., Yagi, T., Kondo, T., and Funamori, N. (1998) Analytical electron microscopy of the garnet-perovskite transformation in a laser-heated diamond anvil cell. In M.H. Manghnani and T. Yagi, Eds., *Properties of Earth and planetary materials at high pressure and temperature*, p. 409–417. American Geophysical Union, Washington, D.C.
- Hirose, K. (2006) Postperovskite phase transition and its geophysical implications. *Reviews of Geophysics*, 44, RG3001, DOI: 10.1029/2005RG000186.
- Hirose, K. and Fei, Y. (2002) Subsolvus and melting phase relations of basaltic composition in the uppermost lower mantle. *Geochimica Cosmochimica Acta*, 66, 2099–2108.
- Hirose, K. and Sinmyo, R. (2007) Partitioning of iron between lower mantle minerals. *Eos Transactions American Geophysical Union*, 88(52), Fall Meeting Supplement, Abstract MR23D-01.
- Hirose, K., Takafuji, N., Sata, N., and Ohishi, Y. (2005) Phase transition and density of subducted MORB crust in the lower mantle. *Earth and Planetary Science Letters*, 237, 239–251.
- Holmes, N.C., Moriarty, J.A., Gathers, G.R., and Nellis, W.J. (1989) The equation of state of platinum to 660 GPa (6.6 MBar). *Journal of Applied Physics*, 66, 2962–2967.
- Ito, E., Kubo, A., Katsura, T., and Walter, M.J. (2004) Melting experiments of mantle materials under lower mantle conditions with implications for magma ocean differentiation. *Physics of the Earth and Planetary Interiors*, 143–144,

- 397–406.
- Kobayashi, Y., Kondo, T., Ohtani, E., Hirao, N., Miyajima, N., Yagi, T., Nagase, T., and Kikegawa, T. (2005) Fe-Mg partitioning between (Mg,Fe)SiO₃ post-perovskite, perovskite, and magnesiowüstite in the Earth's lower mantle. *Geophysical Research Letters*, 32, L19301, DOI: 10.1029/2005GL023257.
- Lauterbach, S., McCammon, C.A., van Aken, P., Langenhorst, F., and Seifert, F. (2000) Mössbauer and ELNES spectroscopy of (Mg,Fe)(Si,Al)O₃ perovskite: A highly oxidized component of the lower mantle. *Contributions to Mineralogy and Petrology*, 138, 17–26.
- Lay, T. and Garnero, E.J. (2007) Reconciling the post-perovskite phase with seismological observations of lowermost mantle structure. In K. Hirose, J. Brodholt, T. Lay, and D. Yuen, Eds., *Post-perovskite: The last mantle phase transition*, p. 129–153. American Geophysical Union, Washington, D.C.
- Mao, W.L., Shen, G., Prakapenka, V.B., Meng, Y., Cambell, A.J., Heinz, D., Shu, J., Hemley, R.J., and Mao, H.-K. (2004) Ferromagnesian postperovskite silicates in the D'' layer of the earth. *Proceedings of the National Academy of Sciences*, 101, 15867–15869.
- Murakami, M., Hirose, K., Kawamura, K., Sata, N., and Ohishi, Y. (2004) Post-perovskite phase transition in MgSiO₃. *Science*, 304, 855–858.
- Murakami, M., Hirose, K., Sata, N., and Ohishi, Y. (2005) Post-perovskite phase transition and crystal chemistry in the pyrolitic lowermost mantle. *Geophysical Research Letters*, 32, L03304, DOI: 10.1029/2004GL021956.
- Nishio-Hamane, D., Fujino, K., Seto, Y., and Nagai, T. (2007) Effect of the incorporation of FeAlO₃ into MgSiO₃ perovskite on the post-perovskite transition. *Geophysical Research Letters*, 34, L12307, DOI: 10.1029/2007GL029991.
- Oganov, A.R. and Ono, S. (2004) Theoretical and experimental evidence for a post-perovskite phase of MgSiO₃ in Earth's D'' layer. *Nature*, 430, 445–448.
- Ohta, K., Onoda, S., Hirose, K., Simmyo, R., Shimizu, K., Sata, N., Ohishi, Y., and Yasuhara, A. (2008a) The electrical conductivity of post-perovskite in Earth's D'' layer. *Science*, 320, 89–91.
- Ohta, K., Hirose, K., Lay, T., Sata, N., and Ohishi, Y. (2008b) Phase transitions in pyrolite and MORB at lowermost mantle conditions: Implications for a MORB-rich pile above the core-mantle boundary. *Earth and Planetary Science Letters*, 267, 107–117.
- Ono, S. and Oganov, A.R. (2005) In situ observations of phase transition between perovskite and CaIrO₃-type phase in MgSiO₃ and pyrolitic mantle composition. *Earth and Planetary Science Letters*, 236, 914–932.
- Ono, S. and Ohishi, Y. (2005) In situ X-ray observation of phase transformation in Fe₂O₃ at high pressures and high temperatures. *Journal of Physics and Chemistry of Solids*, 66, 1714–1720.
- Ozawa, H., Hirose, K., Mitome, M., Bando, Y., Sata, N., and Ohishi, Y. (2008) Chemical equilibrium between ferropericlaase and molten iron to 134 GPa and implications for iron content at the bottom of the mantle. *Geophysical Research Letters*, 35, L05308, DOI: 10.1029/2007GL032648.
- Shieh, S.R., Duffy, T.S., Kubo, A., Shen, G., Prakapenka, V.B., Sata, N., and Hirose, K. (2006) Equation of state of the postperovskite phase synthesized from a natural (Mg, Fe)SiO₃ orthopyroxene. *Proceedings of the National Academy of Sciences*, 103, 3039–3043.
- Simmyo, R., Hirose, K., O'Neill, H.St.C., and Okunishi, E. (2006) Ferric iron in Al-bearing post-perovskite phase. *Geophysical Research Letters*, 33, L12S13, DOI: 10.1029/2006GL025858.
- Simmyo, R., Ozawa, H., Hirose, K., Yasuhara, A., Endo, N., Sata, N., and Ohishi, Y. (2008) Ferric iron content in (Mg,Fe)SiO₃ perovskite and post-perovskite in the deep lower mantle conditions. *American Mineralogist*, in press.
- Stackhouse, S., Brodholt, J.P., and Price, G.D. (2006) Elastic anisotropy of FeSiO₃ end-members of the perovskite and post-perovskite phases. *Geophysical Research Letters*, 33, L01304, DOI: 10.1029/2005GL023887.
- Takafuji, N., Hirose, K., Mitome, M., and Bando, Y. (2005) Solubilities of O and Si in liquid iron in equilibrium with (Mg,Fe)SiO₃ perovskite and the light elements in the core. *Geophysical Research Letters*, 32, L06313, DOI: 10.1029/2005GL022773.
- Tateno, S., Hirose, K., Sata, N., and Ohishi, Y. (2005) Phase relations in Mg₃Al₂Si₂O₁₂ to 180 GPa: effect of Al on post-perovskite phase transition. *Geophysical Research Letters*, 32, L15306, DOI: 10.1029/2005GL023309.
- (2007) High solubility of FeO in perovskite and the post-perovskite phase transition. *Physics of the Earth and Planetary Interiors*, 160, 319–325.
- Zhang, F. and Oganov, A.R. (2006) Valence state and spin transition of iron in Earth's mantle silicates. *Earth and Planetary Science Letters*, 249, 436–443.

MANUSCRIPT RECEIVED APRIL 17, 2008

MANUSCRIPT ACCEPTED MAY 15, 2008

MANUSCRIPT HANDLED BY BRYAN CHAKOUMAKOS